

# TOWARDS THE ADVANCED DEMAND RESPONSE IN DISTRIBUTION NETWORK

Jelena PONOČKO, The University of Manchester, UK  
Jovica V. MILANOVIĆ, The University of Manchester, UK

## SUMMARY

The development of smart grids has introduced many new technologies in the power network, especially at the distribution level. Distributed generation, numerous large electric loads (electric vehicles), demand response, etc., will bring new challenges for the distribution network operator (DNO), primarily in the domain of network flexibility. This paper proposes a methodology for advanced demand response (DR) in the distribution network, catering at the same time for the requirements of the DNO, the available flexibility of the demand side, and the preservation of network performance. Experience has shown the importance of distribution system voltage stability for sub-transmission and transmission system stability. The steady state voltage stability index, namely the load margin, is therefore chosen in this paper as the network performance indicator. This indicator is evaluated before and after a DR action, in order to analyse the possible effect of DR on network stability. The DR program can then be “tailored” to meet the requirements of the DNO (e.g. load curtailment) and keep the voltage stability of the network. Optimisation is first performed with the objective of “flattening” the day-ahead forecasted total loading at the GSP during a 24 hour period, i.e. perform peak shaving and valley filling, taking into account forecasted aggregated flexibility of the distribution network buses. In the second step, DR is adjusted in case the voltage stability index is violated in some of the time steps of the planning horizon (24 h). The suggested approach takes into account load pay-back, i.e. gradual increase of load at time steps following a DR action, where controllable load is (fully or partly) shifted from one period of the day to another.

**Key words:** demand response, load modelling, optimisation, voltage stability

{jelena.ponocko; milanovic}@manchester.ac.uk

## INTRODUCTION

With the evolution of renewable energy sources and distributed generation, network operation is shifting towards the demand side. In order to meet the volatility of the renewable sources, the flexibility of the demand side can be harnessed instead of costly generation units with fast ramping. The activation of the demand side is necessary to follow the variability of the distributed generation and/or meet the distribution network operator’s (DNO’s) requirements (maintaining network reliability or reducing the cost of supply[1]). Demand side management, namely demand response (DR) at the distribution network level, can therefore play an important role in the ancillary services provided to the transmission network at the grid supply point (GSP). As the penetration of distributed energy resources (DER) becomes concentrated in certain areas, it may have an increased effect on sub-transmission and transmission levels[2]. The same applies to the aggregation of flexible end-users providing DR. An advantage of aggregated load control is that variations of a large number of small devices are smaller than variations of a small number of large devices (i.e. generators), whose failure would therefore have a larger effect on the grid than the rejection of small devices [3]. The network operator should therefore consider controlling the aggregate DER, including distributed generation, storage and DR providers.

National Grid (the UK transmission system operator) has set a goal of 30–50% of balancing capability from demand side sources by 2020 [4]. Balancing services (reducing/increasing/shifting load consumption), with response within minutes, will be enabled via aggregators. Currently 80% of DR customers are contracted via an aggregator, although some also contract directly with the National Grid (20%) or through their DNO (10%). Currently around 350 MW of load reduction is procured from DR participants in the UK, while an Ofgem survey[4] reports that there is a far greater untapped flexibility potential (around 3GW for reducing demand and around 2GW for increasing demand).

As the changes in DER at distribution level may influence the transmission network, the network performance indicators (such as frequency and voltage stability) should be recorded and kept unchanged (if not improved)

during and after control actions. For example, voltage instability in the distribution system, also referred to as load instability, can spread to the transmission system and cause a major blackout [5]. During a heavily loaded condition, even a relatively small but sudden increase in demand can result in voltage instability [6]. If the current operating point is at the upper half of the PV curve (also known as the “nose curve”, given in Fig. 1a), the active power (P) margin is the amount of load increase that will cause the power system to reach voltage (V) limit. In case of contingencies, the PV curve will change, resulting in a lower P margin even at the same operating point.

As most distribution networks have one voltage regulation point, i.e. the GSP [5], this paper introduces a methodology for advanced DR in a distribution network connected to the transmission network at one GSP. The advancement relies on three key points: i) the observability of the demand side is enhanced by monitoring consumption of each electrical appliance at a limited number of end-users’ premises; ii) the DR program can be planned by taking into account the forecasted flexibility of the aggregate demand; iii) voltage stability is chosen as the network performance indicator – this indicator is assessed before a DR action, and should not be deteriorated after a DR action. The DR program is thus tailored to meet the requirements of the DNO (e.g. load curtailment) and cater for the voltage stability of the network. The paper analyses how shifting different types of load (disconnecting them at one time step, and reconnecting them at a later time) can affect the voltage stability. The methodology is equally applicable to residential, commercial, industrial or mixed sectors.

## LOAD MODELLING

Following the three previously mentioned key points of an advanced DR program, load scheduling can be planned, e.g. a day ahead, based on the forecasted demand flexibility at each load bus and taking into account the effect of load changes on the network performance, namely the voltage stability index (VSI). VSI in this paper is given as the load margin (in MW). The load margin represents the critical load increase in the network (starting from the current operating point  $P_0$ ) which leads to the voltage collapse (critical) point, as depicted in Fig. 1a. An accurate voltage stability analysis requires an appropriate load model, taking into account the types of load that are voltage dependent, and those that are not.

In order to represent the demand side as realistically as possible, and assess the voltage stability, the load is modelled using a composite load model consisting of a polynomial (ZIP) model connected in parallel with an induction motor (IM) model [7], as shown in Fig 1b. The ZIP model is described by equations (1) and (2):  $P_L$  and  $Q_L$  are active and reactive demand at a load bus at voltage value  $V$ ;  $a$ ,  $b$  and  $c$  refer to the share of constant power, constant current and constant impedance components of the load, respectively, while  $P_{L0}$  and  $Q_{L0}$  refer to the active and reactive demand at the nominal voltage  $V_0$ .

$$P_L = P_{L0} \left[ a_P + b_P \left( \frac{V}{V_0} \right) + c_P \left( \frac{V}{V_0} \right)^2 \right] \quad (1)$$

$$Q_L = Q_{L0} \left[ a_Q + b_Q \left( \frac{V}{V_0} \right) + c_Q \left( \frac{V}{V_0} \right)^2 \right] \quad (2)$$

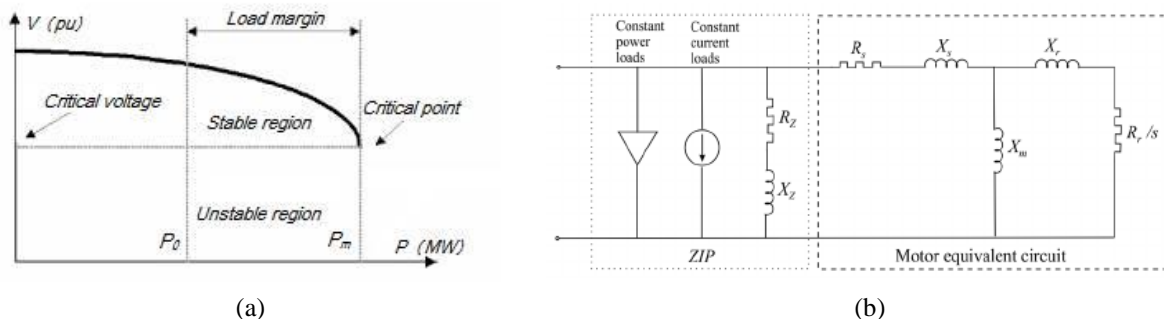


Fig. 1 PV curve (a) and composite ZIP+IM load model (b)

Detailed modelling of demand is only possible when information about demand composition is available. This methodology relies on the existence of smart meters and sub-metering technologies. Smart meters in this approach are assumed to be reporting the active and reactive consumption of each home appliance, at least every 30 minutes, enabling information about real-time and, consequently, forecasted aggregated demand composition (shares of controllable and uncontrollable loads) at each bus. An approach for decomposing total demand at the

aggregation point (e.g. a substation) was suggested in [8], where the composition of the aggregate demand can be forecasted based on historical smart meter data (including sub-metering measurements) and the total demand forecast. With this approach, six load categories have been identified in the residential demand sector, as shown in Table 1: single-phase constant torque induction motors (CTIM1), single-phase quadratic torque induction motors (QTIM1), controllable resistive loads ( $R_C$ ), uncontrollable resistive loads ( $R_{UC}$ ), switch-mode power supply (SMPS) loads and Lighting. Furthermore, the categories are grouped into controllable and uncontrollable, based on their suitability for DR.

TABLE 1 – LOAD CATEGORIES AND CORRESPONDING TYPES OF APPLIANCE

Controllable		Uncontrollable	
Load categories	Residential appliances	Load categories	Residential appliances
CTIM1	HVAC, dish washer, tumble dryer, washing machine, washer-dryer, vacuum cleaner	$R_{UC}$	Iron, hob, oven
QTIM1	Chest freezer, fridge-freezer, fridge, upright freezer	SMPS	Answer machine, CD player, Clock, telephone, high fidelity (HiFi) appliances, Fax machine, PC, printer, TV, VCR-DVD, receiver, microwave
$R_C$	Water heater, electrical shower, storage heater, electrical space heating	Lighting	Lighting

Assuming that there is a limited number of SMs with sub-metering capabilities, the methodology in [8] relies on artificial neural networks, which were trained with available per-appliance monitoring data, and used to forecast, day ahead, the composition of the aggregated demand. The results showed that even with 5% of the aggregated demand being monitored at appliance level, it is possible to estimate the composition of the overall demand with an accuracy of 95%. Demand composition can be presented as the shares of different load categories within the total daily loading curve, as illustrated in Fig. 2. Fig. 2a represents the demand composition of active demand, while Fig. 2b represents the reactive demand composition.

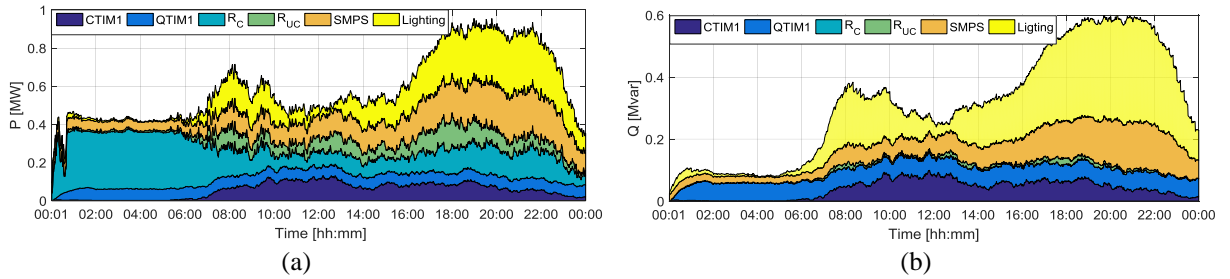


Fig. 2 Demand composition of: (a) active and (b) reactive demand

Once the information about demand composition is available, one can proceed to modelling the demand using the ZIP+IM (composite load) model, following the classification of load categories into ZIP+IM components, as given in Table 2. Constant Z loads have a controllable and an uncontrollable component, while other types are either controllable (IMs) or uncontrollable (constant I and constant P). The main types of appliance participating in DR are therefore water and space heating devices, HVAC (heating, ventilation and air conditioning) units and washing/drying machines.

TABLE 2 – ZIP+IM LOAD MODEL COMPONENTS AND CORRESPONDING LOAD CATEGORIES

ZIP+IM model component	Load category
$Z_C$ (controllable constant impedance loads)	$R_C$
$Z_{UC}$ (uncontrollable constant impedance loads)	$R_{UC}$
I (uncontrollable constant current loads)	Lighting
P (uncontrollable constant power loads)	SMPS
IM (controllable induction motors)	CTIM1+QTIM1

Different flexibility of demand at different buses is taken into account, together with the variation of flexibility in time, following the hourly changes in the end-users' consumption. Demand at each bus is divided into its controllable and uncontrollable part, based on the assumed availability of smart meter data and sub-metering measurements. Therefore, following a DR request and direct load control scenario, load can only be curtailed/shifted as much as its controllable part allows. Consequently, information about forecasted demand

composition and demand controllability reduces uncertainty in the actual result of the DR program, but also of the voltage stability assessment.

## METHODOLOGY

The main steps of the proposed methodology are given in Fig. 3. Based on the predefined loading curve at the substation point, requested by the DNO or the transmission system operator, the algorithm optimizes the load dispatch (i.e. load shift) across the flexible load buses in such a way that the voltage stability index (here, critical distribution network loading) is not drastically reduced after the DR action. In other words, the load dispatch is performed both to enable demand reduction (within the given flexibility limits) and maintain/improve network performance with respect to steady state voltage stability. The DR is planned day ahead (as in [9]), taking into account the forecasted daily loading curve (DLC) and the available controllable load, based on the information about load composition.

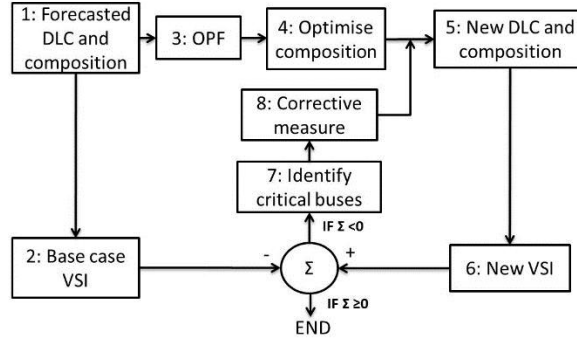


Fig. 3 Flowchart of the methodology

As a first step, the optimal power flow (OPF) is run, with the main objective of following a predefined loading curve. Although there are various objectives of load scheduling, e.g., peak shaving, load shaping or contingency load shedding [10], the objective function in this analysis is to flatten the DLC, i.e., to minimise the peak-to-average ratio, following the approach given in [11, 12]. This is performed by the so called peak clipping and valley filling, which aim at reducing the difference between peak and valley load levels, resulting in increased security of the grid [9]. As a result, the main output of the OPF is a new DLC and a new load composition at each load bus and at each time step.

### Optimal power flow (step 3 of the flowchart)

The basic optimisation problem of the OPF, minimising the generation cost, is given as follows:

$$\min \sum_{j=1}^{N_G} C_j P_{G,j}, \quad (3)$$

where  $C_j$  is the generation cost of generator  $j$ , and  $P_{G,j}$  is its power output. The following equality and inequality constraints of the OPF are taken into account at each time step:

- Load flow equations [13]:

$$P_{G,i} - P_{D,i} = V_i \sum_{k=1}^N V_k [G_{ik} \cos \theta_{ik} + B_{ik} \sin \theta_{ik}] \quad (4)$$

$$Q_{G,i} - Q_{D,i} = V_i \sum_{k=1}^N V_k [G_{ik} \sin \theta_{ik} - B_{ik} \cos \theta_{ik}], \quad (5)$$

where  $i$  is the bus number,  $G$  and  $B$  are the real and imaginary parts of the admittance matrix,  $P_{G,i}$  is the generation in bus  $i$  and  $P_{D,i}$  is the demand in bus  $i$ .

- Bus voltage limits:

$$V_i^{MIN} \leq V_i \leq V_i^{MAX} \quad (6)$$

- The maximum line loading (MVA) is neglected due to the commonly oversized lines in the distribution network.
- Generation limits:

$$P_{G,i}^{MIN} \leq P_{G,i} \leq P_{G,i}^{MAX} \quad (7)$$

- Network losses are minimised using the slack bus approach [14], where the slack bus active generation is minimised (by enforcing a high generation cost).
- At each time step  $t$ , the demand  $P_D$  at each bus  $i$  is recalculated as follows:

$$P_{D,i,t} = \text{forecasted}_{i,t} - \text{disconnected}_{i,t} + \text{connected}_{i,t} \quad (8)$$

Connected load refers to the load payback at time  $t$ . Load payback represents the reconnection of the disconnected loads, which appears in the time steps following the disconnection. There are various ways to model load payback [15, 16]. In this paper, load payback of the constant  $Z$  loads is modelled as a linear increase of load [16], represented by the following equation:

$$PB(t) = \alpha \cdot [\Delta(t-1) + \Delta(t-2)] + \beta \cdot [\Delta(t-3) + \Delta(t-4)] + \gamma \cdot [\Delta(t-5) + \Delta(t-6)], \quad (9)$$

where  $PB(t)$  is the payback load at time step  $t$ ,  $\Delta$  is the amount of curtailed load (in MW), and  $\alpha$ ,  $\beta$  and  $\gamma$  are the payback coefficients for load curtailed in the six preceding time steps. Here,  $\alpha$ ,  $\beta$  and  $\gamma$  are chosen to be: 0.25, 0.2 and 0.05, respectively. Since the sum of these coefficients equals 1 over the six time steps, it is assumed that all the constant Z loads will be reconnected within the three hours following the disconnection. Thus, 50% of the disconnected loads will be reconnected in the first hour, following 40% in the second hour and the last 10% in the third. Other approaches can also be taken. Regarding the induction motor (IM) loads (usually HVAC units and washing/drying machines), it is assumed that the users/aggregator are given freedom to choose when to reconnect the machines, as long as it is during the valley periods (mostly night time, between midnight and 7 am). During the valley period, the load is lower than the one requested by the network operator. Therefore, the IMs are reconnected randomly, within the given periods of time. These two payback models account for the end-users' commodity - they consider the usage of heaters as more comfort-constrained, i.e. end-users are more tolerant about postponing the washing of their laundry/dishes than to waiting for hot water. Similar availability of these load types was reported in [10].

#### **Optimisation of demand composition (step 4 of the flowchart)**

DR is planned in such a way to meet the requirements of the network operator, but also to keep the demand composition as close as possible to the original. This scenario is more realistic than the one where only one load type is being shifted across many users, as different users will be more prone to delay operation of different types of appliance. Demand composition has also been recognised as an important factor in dynamic response of demand, which occurs after a disturbance in the network and influences the voltage and angular stability of the system [17]. Thus, both the load shift and load payback are planned to keep the demand composition almost unchanged. If the load control is executed from a central control point, a matching number of IM or Z loads is disconnected in one time step and reconnected in another, making sure that the shares of these load categories remain similar to the ones before DR. This is done in each time step and for each individual bus, by performing a linear least square optimisation, using information given by the OPF output on the amount of load that has to be shifted at each bus ( $P_{Shifted}$ ). The objective function, given by (10a), implies that the sum of disconnected IM and Z loads has to be as close as possible to the required amount of shifted load ( $P_{Shifted}$ ).

$$\min (P^Z_{Disconnected} + P^{IM}_{Disconnected} - P_{Shifted})^2 \quad (10a)$$

$$\text{subject to: } \frac{\Delta IM}{P_0} = \frac{\Delta IM - P^{IM}_{Disconnected} + P^{IM}_{Connected}}{P_0 - (P^Z_{Disconnected} + P^{IM}_{Disconnected}) + P_{Connected}} \quad (10b)$$

$$0 \leq P^Z_{Disconnected} \leq \Delta Z ; \quad 0 \leq P^{IM}_{Disconnected} \leq \Delta IM \quad (10c)$$

Equality constraint (10b) suggests that the share of IMs in the total demand after the DR should be the same as the one before DR action.  $\Delta IM$  is the amount of controllable IMs (in MW),  $P^{IM}_{Disconnected}$  is the amount of shifted IMs, and  $P^{IM}_{Connected}$  is the payback load of the IMs. Inequality constraints (10c) limit the load shift by the amount of controllable loads at the respective bus and time step. Finally, we can conclude that the OPF informs us how much load should be shifted at each load bus and each time step ( $P_{Shifted}$ ), while the proposed optimisation process tells us how much of which type of load should and can be shifted ( $P^Z_{Disconnected}$ ,  $P^{IM}_{Disconnected}$ ). The former uses information about the total controllable demand, while the latter uses information about the amount of controllable load categories (IM and Z).

Two cases of DR approach are examined in this paper:

- i. Case 1: Every time load is disconnected, the amount of disconnected IM loads is resolved using the optimisation process, as given by the equality constraint (1a), and controllable constant Z loads are disconnected only if the objective loading curve is not met.
- ii. Case 2: Similar to case 1, but in this case constant Z loads are disconnected first, which means that  $\Delta Z$  and  $P^Z$  will participate in equation (9b) instead of  $\Delta IM$  and  $P^{IM}$ , respectively.

Considering that IM loads work for approximately one hour (some shorter, and some longer than that), if certain load is shifted in one time step, the amount of flexible load in the following time step gets smaller by the amount of the shifted load. This simplified approach illustrates the subsequent changes in flexibility when loads with a longer operational time are disconnected. Constant Z loads are considered to be operating for no longer than half an hour (one time step), which is why their shift at the one time step does not affect the controllability in the next time step.

### VSI assessment and correction (steps 6- 8 of the flowchart)

Once the load scheduling is planned, VSI is assessed with the new network conditions (new loading curve and load composition at each bus). In order to account for the composite load model in the steady state voltage stability evaluation, DigSILENT Power Factory 15.2 [18] was used due to its ability to incorporate realistic load models. (Note: Otherwise, for the commonly used constant power load model, Matpower's continuation power flow can be performed). The so called "PV curve" simulations were performed for 48 time steps (24 h planning horizon) using Matlab and Python interfaces with DigSILENT. In these simulations, demand at all buses is gradually increased until the load flow becomes infeasible – the last operating point, i.e., the maximum network load providing a feasible load flow is saved as the critical loading point. The distance between the original operating point  $P_0$  (total network load) and the critical one ( $P_m$ ) is represented by the load margin (VSI), as depicted in Fig. 1a.

If, in some time steps of the planning horizon, the VSI after DR appears to be lower than before DR, the load dispatch (shift) is changed in the corresponding time steps. A common approach would be to apply changes only to the critical buses, which are those with the highest (absolute) sensitivity of bus voltage to the total network load increase ( $dV/dP$ ) in all the observed time steps. At these buses, all the flexible demand (including IM and controllable Z loads) can be shifted in the time steps where the VSI is lower. This corrective measure can be performed once, or iteratively, until a satisfactory VSI limit is obtained.

### CASE STUDY

The network used in this paper is the slightly modified IEEE 33 bus distribution network (Fig. 4). Bus 1 is taken as the generator bus with a fixed active power output, serving as the objective value for the total load. Bus 34 is the slack bus, representing the GSP, and covers the mismatch between the available generation on one side, and load and network losses on the other. All the 32 load buses are considered flexible, and each load bus has a different DLC and demand composition during the day. Each flexible load bus in the network model represents a secondary substation supplying around 50 residential end-users. The default load values for the network buses (active and reactive power in the IEEE model) are taken as the maximum daily values. The assigned DLC and demand composition are generated using the CREST load model [19], as detailed in [8]. The added line 2-34 has the same impedance as line 1-2, while line 34-19 has the same impedance as line 19-20.

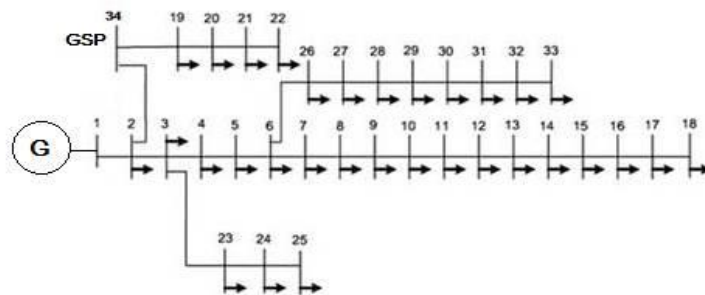


Fig. 4 Modified IEEE 33 bus network

The OPF is run in Matpower[20] to meet the desired loading curve. As some of the typical aims of DSM are to maximise the use of renewables and minimise the energy import from the main grid, the OPF in this example tends to adjust the flexible loads to the available generation, and minimise the active flow through the slack bus (GSP). The flat loading curve, as the objective of the DR, is enforced by fixing the active power output of the generator in bus 1 to the mean value of the base case loading curve (illustrated as a horizontal dotted line in Fig 5 (top)). In this example, the mean equals 1.85 MW. Matpower allows the modelling of flexible loads as distributed generators with negative power output, where the negative generation limits are enforced by load controllability ( $P_{G,i}^{MIN} = -P_{D,i}$  and  $P_{G,i}^{MAX} = -P_{D,i} + P_{controllable}$ ). It should be noted that only a constant power load model is available in this software. As the objective function of the OPF is to minimise the generation cost, the generation following (instead of conventional load following, where the generation is adjusted to the load demand) is accomplished by adding a high cost to the slack generator, so that the flexible loads adjust to the predefined loading curve (in this case, flat load of 1.85 MW). This allows the flexible demand to follow the available flat generation, and the losses to be minimised. The OPF is run for 48 consecutive time steps, where every time step corresponds to a 30 minute period (24 h in total).

## RESULTS

The load scheduling results are given in Fig. 5 (top). The OPF meets the objective (Pref), constrained by the available demand flexibility, load payback and preservation of demand composition. DR in case 1 (prioritising IM in the optimisation process given by equations (9a-9d)) results in a higher load than case 2 due to the load payback, as well as the reduced flexibility of IM loads in time steps succeeding those where IM were shifted. Even though the load peak is reduced, and load valleys filled, the load margin is lower after the DR at certain time steps (e.g. before 08:00 and 10:00), as illustrated in Fig. 5 (bottom). Although one would expect that with a reduced loading curve the VSI would increase, it actually decreases.

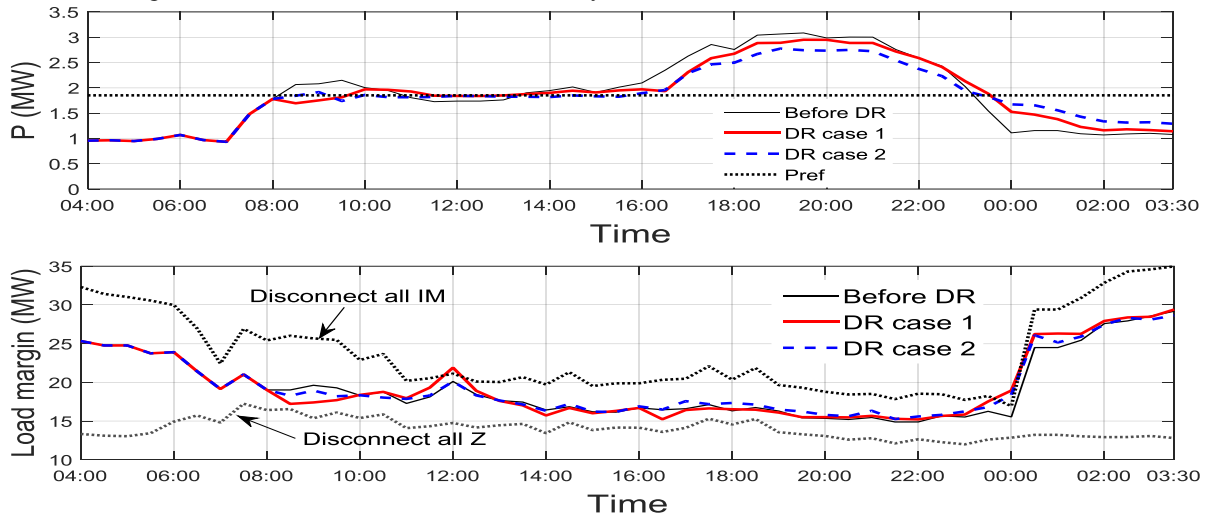


Fig. 5 DLC before and after DR (top) and the resulting loadmargin (bottom)

The obtained demand composition (where 1 p.u. corresponds to total demand in each time step) can be observed in Fig. 6. Even though the total demand changes, the shares of the load components of the ZIP+IM model stay almost the same. Due to the preservation of the demand composition, however, the flexibility of demand was not entirely exploited.

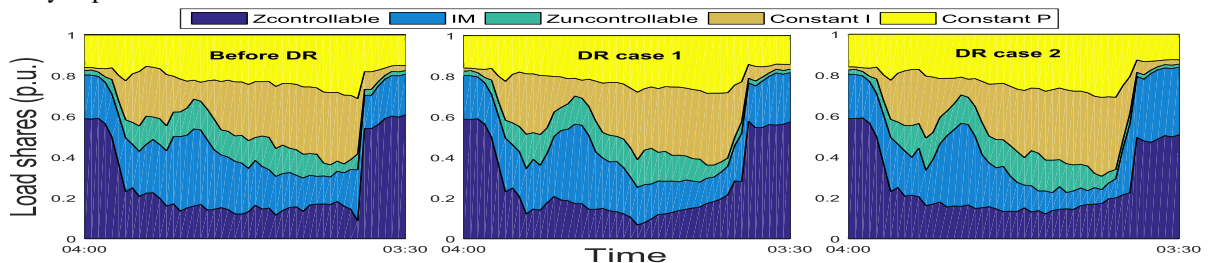


Fig. 6 Demand composition before and after DR

Before proceeding to any corrective action, the threshold for deciding the network performance with respect to VSI should be established. Even though in some time steps the new VSI may be lower than the original one, the network performance may still be satisfactory, and no corrective measures should be taken. Let us assume that the voltage stability in the normal operating state, i.e. before any DR action is performed, is the first threshold. This means that any VSI, regardless of the time of day, being lower than the original one, is dangerous for the network. However, if the load margin before the DR action was very high, and it decreases, the system may still be very far from a voltage collapse point. A more realistic approach would be setting the single minimum value of the VSI in the base case as the threshold. That would mean that the new loading curve (and demand composition) should not cause a load margin lower than the minimum one from the base case. In this example, the minimum load margin before the DR was about 15 MW.

The nose points (voltage collapse points) for the most critical bus in the network (bus 18) are depicted in Fig. 7. In the base case, i.e. case before DR, the critical system loading during the observed 24 hour is between 15 MW and 30 MW, approximately. It can be seen that the DR cases 1 and 2 do not “step outside” this stability “cloud”. In other words, after applying DR, in all the time steps the nose point is within the values given in the base case. However, in marginal cases, if all the IM loads or all the Z loads were curtailed, with no payback, the “cloud” moves drastically. These marginal examples were illustrated in Fig.5 (bottom) as dotted lines. Disconnecting all

the constant Z loads deteriorates the stability zone, and moves it towards lower system loading. On the other hand, disconnecting all the IM loads improves the voltage stability at some time steps, increasing the total loading to more than 35 MW. It can be concluded that, as long as the critical points are within the base case zone, no corrective measures should be taken.

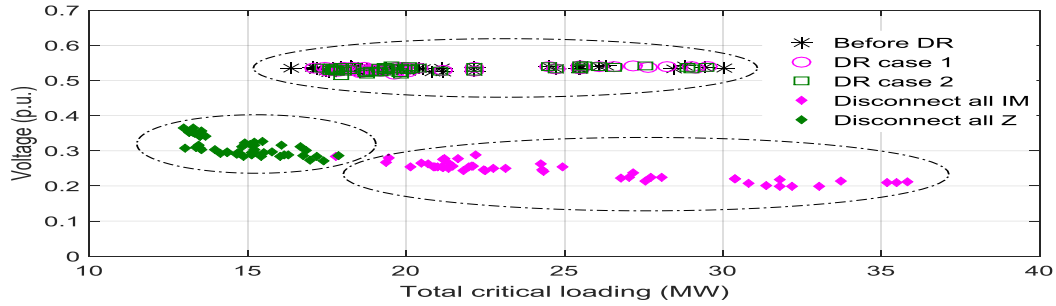


Fig.7 Voltage collapse zones before and after DR

Table 3 illustrates the number of time steps (out of 48 steps in total) where the VSI was violated after the DR action, following different thresholds (minimum VSI from the base case, and 99%, 98% and 95% of the time changing values of the VSI) and the two DR cases, before and after corrective measures for improving the VSI. It can be seen that the minimum load margin was not violated at any time step, while, depending on other thresholds, the number of critical time steps ranged between 17 and 4 for DR case 1, and between 11 and 1 for DR case 2. After the corrective measure (all the flexible loads are shifted) was applied to the critical buses at the critical time steps, the VSI improved in some cases, resulting in the number of critical time steps ranging between 19 and 1 for case 1, and between 11 and 0 for case 2. Corrective action mostly brings improvements in the case of the first DR approach. The outcome of the corrective measure is rather stochastic due to the load payback and limited load flexibility in some cases.

Finally, a confidence zone for VSI can be established, based on the minimum value of VSI in the base case, and the 95% of the VSI over the time steps, as shown in Fig. 8. In this way, if the new VSI values belong to the favourable zone (above 95% VSI) or permissible zone (less than 95% VSI, but no less than minimum VSI), no corrections are needed. Otherwise, if VSI falls into the critical zone, additional load curtailment can be performed at the critical time steps, and at the critical load buses.

TABLE 3 – NUMBER OF TIME STEPS WITH VSI VIOLATION, BEFORE AND AFTER CORRECTIONS

VSI threshold	DR case 1		DR case 2	
	Before corrections	After corrections	Before corrections	After corrections
VSI <sub>min</sub>	0	/	0	/
VSI	17	19	11	11
0.99VSI	11	9	7	7
0.98VSI	7	5	4	6
0.95VSI	4	1	1	0

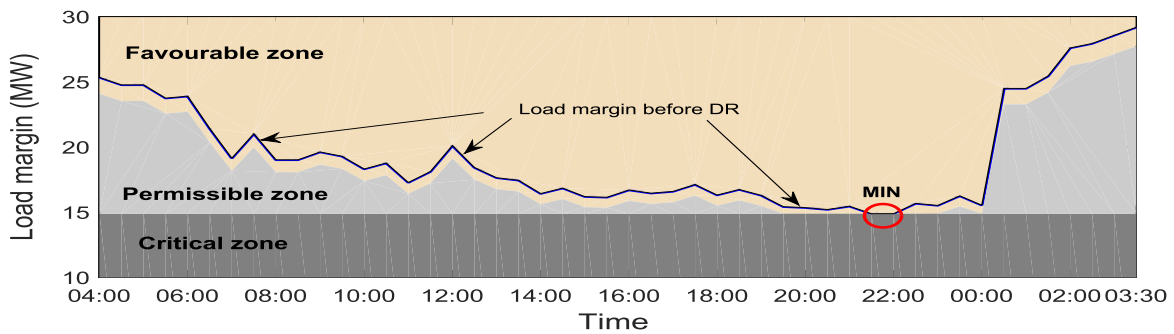


Fig. 8 Voltage stability zones with respect to load margins



## CONCLUSION

This paper presented a methodology for advanced DR, optimising between the distribution/transmission system requirements, availability of demand flexibility, which depends on the composition of demand, and preservation of system stability (in this paper, only steady state analysis is performed). A two level approach has been suggested: at the first step, load scheduling is planned day ahead to meet the daily loading requirements given by the network operator; at the second step, corrective measures are planned, also day ahead, for the time steps where the DR output results in a violated voltage stability compared to the network conditions before the DR. The optimization results can be used not only to assess the extent to which the aforementioned objectives and constraints have been met, but also to investigate the possible monetary or other types of incentive necessary in cases where the available DR is insufficient and more end-users should be attracted to participate in demand curtailment/shifting.

## ACKNOWLEDGMENTS

This research is supported by the EU Horizon 2020 project "NOBELGRID", contract number 646184.

## LIST OF REFERENCES

- [1] I. Cobelo, "Active Control of Distribution Networks," PhD thesis, School of Electrical and Electronic Engineering, The University of Manchester, 2005.
- [2] "The Integrated Grid - Realizing the Full Value of Central and Distributed Energy Resources," EPRI, 2014.
- [3] D. S. Callaway and I. A. Hiskens, "Achieving controllability of electric loads," *Proceedings of the IEEE*, vol. 99, pp. 184-199, 2011.
- [4] "Demand Side Flexibility Annual Report 2016 - Power Responsive," National Grid, 2016.
- [5] A. Jalali and M. Aldeen, "Modified modal analysis approach for distribution power systems," in *Innovative Smart Grid Technologies Conference Europe (ISGT-Europe), 2017 IEEE PES*, 2017, pp. 1-6.
- [6] Y. Zhu, "Ranking of Power System Loads Based on Their Influence on Power System Stability," The University of Manchester, 2016.
- [7] X. Tang and J. V. Milanović, "Assessment of the impact of demand side management on power system small signal stability," in *2017 IEEE Manchester PowerTech*, 2017, pp. 1-6.
- [8] J. Ponocko and J. V. Milanovic, "Forecasting Demand Flexibility of Aggregated Residential Load Using Smart Meter Data," *IEEE Transactions on Power Systems*, vol. PP, pp. 1-1, 2018.
- [9] T. Logenthiran, D. Srinivasan, and T. Z. Shun, "Demand Side Management in Smart Grid Using Heuristic Optimization," *IEEE Transactions on Smart Grid*, vol. 3, pp. 1244-1252, 2012.
- [10] B. P. Hayes, "Distributed generation and demand side management: Applications to transmission system operation," 2013.
- [11] A. Brooks, E. Lu, D. Reicher, C. Spirakis, and B. Wehl, "Demand Dispatch," *IEEE Power and Energy Magazine*, vol. 8, pp. 20-29, 2010.
- [12] A. H. Mohsenian-Rad, V. W. S. Wong, J. Jatskevich, R. Schober, and A. Leon-Garcia, "Autonomous Demand-Side Management Based on Game-Theoretic Energy Consumption Scheduling for the Future Smart Grid," *IEEE Transactions on Smart Grid*, vol. 1, pp. 320-331, 2010.
- [13] N. Rajaković, *Analiza elektroenergetskih sistema II: Akademska misao, Elektrotehnički fakultet Beograd*, 2008.
- [14] J. A. Momoh, *Electric power system applications of optimization*, Marcel Dekker, Inc., 2001.
- [15] M. Ziaii, A. Kazemi, M. Fotuhi-Firuzabad, and M. Parvania, "A method to calculate the linear load pay back factors for air conditioners," in *Power and Energy Engineering Conference (APPEEC), 2012 Asia-Pacific*, 2012, pp. 1-5.
- [16] H. Kun-Yuan and H. Yann-Chang, "Integrating direct load control with interruptible load management to provide instantaneous reserves for ancillary services," *IEEE Transactions on Power Systems*, vol. 19, pp. 1626-1634, 2004.
- [17] Y. Xu and J. V. Milanović, "Day-Ahead Prediction and Shaping of Dynamic Response of Demand at Bulk Supply Points," *IEEE Transactions on Power Systems*, vol. 31, pp. 3100-3108, 2016.
- [18] F. Gonzalez-Longatt and J. L. R. Torres, "Advanced Smart Grid Functionalities Based on PowerFactory," ed: Springer, 2017.
- [19] I. Richardson, M. Thomson, D. Infield, and C. Clifford, "Domestic electricity use: A high-resolution energy demand model," *Energy and Buildings*, vol. 42, pp. 1878-1887, 2010.
- [20] R. D. Zimmerman and C. E. Murillo-Sánchez, "Matpower 6.0 User's Manual," ed: December, 2016.